Available online at www.sciencedirect.com
SCIENCE DIRECT®
Computers and Chemical Engineering 29 (2005) 2386–2403

CFD analyses of complex flows

Richard Farmer [a,*], Ralph Pike [b], Gary Cheng [c]

[a]
[b]
[c]

Received 11 May 2005; accepted 23 May 2005
Available online 2 September 2005

Ab a

Computational fluid dynamics (CFD) of complex processes and complicated geometries embraces the transport of momentum, heat, and mass including the description of reaction kinetics and thermodynamics. The paper outlines the numerical models available for analyzing these processes and presents examples of such methodology. The unprecedented growth in computer capability has resulted in efficient simulations of most transport phenomena. The aerospace's interest in high-pressure turbulent combustion has created efficient computational tools for analyzing run-away-reactions in the process industries. Practical turbulence models, generalized thermodynamic properties, and extensive chemical kinetics data bases are currently used in three-dimensional, steady-state simulations. However, industrial needs have challenged CFD modelers to improve their flow solvers in order to simulate flows with more complicated physics, such as spray combustion, acoustic waves, transient start-up and shut-down, and flow instabilities. In addition, the practicality and efficiency of numerical simulations are highly dependent on the submodels employed, such as reaction mechanisms and turbulence models. There has been some progress in generalizing CFD tools, but more development is needed. Most of all, more high-quality and critical test data are required to validate the CFD simulations of complex processes. The laminar transport equations have been averaged by various means to locally describe both turbulent and multi-phase flows. Spray combustion, stirred-tank reactors, fluidization of catalytic beds, and highly exothermic supercritical reactors are among the several validated examples, which illustrate today's technology. The designer's access to public-domain, open-source software offers powerful methodology for his use. Such software and the variety of available modeling techniques will be inventoried to demonstrate the scope of computational transport methodology. The current state of CFD models will be assessed to address the need for future research.

Computational transport phenomenon; Process models; Model validation

1. I

Today's computers offer unprecedented computational power to address complex chemical process operational and design issues. However, the practicing engineer's expertise in using this methodology and the availability of more demanding experimental validation data are required to reap the benefit of such simulation methodology. The partial differential equations, which represent turbulent flow and heat transfer were available over a hundred years before practical solution techniques were developed. Still, most process analyses are made with simplistic methods, especially with respect to the treatment of geometric flow variation. This paper outlines the various detailed modeling methods which are in use, and attempts to emphasize their similarities, in order to illustrate the analytical power which is currently within our reach. Specific examples will be presented to show what is possible, if we can effectively separate basic research studies from practical engineering approaches.

* Corresponding author. Tel.: +1 775 883 2417.
farmer@sierraengineering.com (R. Farmer), pike@she.lsu.edu (R. Pike), gcheng@uab.edu (G. Cheng).

0098-1354/$ – see front matter © 2005 Elsevier Ltd. All rights reserved.
doi:10.1016/j.compchemeng.2005.05.022

Computational fluid dynamics (CFD) has been developed primarily to describe the flow of air as an ideal gas and of constant density liquids. The conservation equations of mass, momentum, and energy, when simplified to describe such flows, are solved with a variety of numerical techniques. The complexities arising from including turbulence, fluid property variation and reactions, and multi-phase flows in the simulations have not been addressed in a systematic fashion. However, enough work has been accomplished, and some of it made available as leased computational software that basic computational methodology can be identified. A critique of these models is shown in the following. These models may aptly be called computational transport phenomena (CTP), due to their applicability to multi-component and multi-phase flows. The models are meant to be illustrative only. A definitive critique is not possible due to commercial analytical codes and company codes being proprietary and to the current position of the government being to suppress federally funded research activities.

2. T

Two basic approaches are used to formulate the conservation equations for modeling complex chemical processes. Firstly, a balance on an arbitrary control volume yields the transport equations for the property, Ψ:

$$\frac{\partial \Psi}{\partial t} + \square \cdot (\vec{v}\Psi) = \square \cdot \Omega + \sigma$$

where Ω))

The momentum equation:

$$\frac{\partial \rho \times \bar{U}}{\partial t} + \nabla \cdot \rho \times \bar{U} \times \bar{U} + \nabla \cdot (P \times \hat{I} - \hat{\tau}) - \rho \times \bar{g} \quad d\Omega = 0$$

The thermal energy equation:

$$\frac{\partial \rho \times h \times \bar{U}}{\partial t} + \nabla \cdot (\rho \times h \times \bar{U}) - \frac{\mathrm{D}P}{\mathrm{D}t} + \nabla \cdot \bar{q} - \hat{\tau} : \nabla \bar{U} - \sum_k \bar{j}_k \cdot \bar{g} \quad \mathrm{d}\Omega = 0$$

The species continuity equation:

$$\frac{\partial \rho_i}{\partial t} + \nabla \cdot \rho_i \times \bar{U} + \nabla \cdot \bar{j}_i - \omega_i \quad \mathrm{d}\Omega = 0$$

where

$$\hat{\tau} = +\mu(\nabla \bar{U} + (\nabla \bar{U})^{\mathrm{T}}) - \frac{2}{3}\mu - b \quad (\nabla \cdot \bar{U})\hat{\delta}$$

$$\bar{j}_{\mathrm{im}} = -\rho D_{\mathrm{im}} \nabla \cdot \alpha_i$$

$$\bar{q} = -\kappa \nabla T + \sum_k h_k \times \bar{j}_k$$

and β is the property/unit volume, the number or mass average velocity,

coordinates and ζ's as internal coordinates of the property Ψ. The internal coordinates are used to simulate the physical processes, which the particles are undergoing.

$$\int_R \left[\frac{\partial \Psi}{\partial t} + \sum_{k=1}^{3} \frac{\partial}{\partial x_k}(v_k \times \Psi) + \sum_{j=1}^{m} \frac{\partial}{\partial \zeta_j}(u_j \times \Psi) + D - B \right] d\bar{R} = 0$$

To simplify the simulation, the integration over the internal coordinates was accomplished by using the method of moments. Applications are discussed in Randolph and Larson, . Such methods are still under investigation; Verkoeijen et al., "Population balances for particulate processes: A volume approach," , vol. 57, 2002. As with most chemical process analyses, such research has been primarily directed at investigating the physical processes the particulates are encountering while over simplifying their motion, i.e. assuming the velocity field or restricting its geometric variation.

With a goal of getting more detail into the analysis of turbulent flows, investigators have stopped short of averaging the laminar flow conservation equations to initiate their analyses. Instead, they solve a transport equation for the PDF or approximate the PDF from experimental data. To date, such modeling approaches have not produced practical process simulation models, although they have contributed to a more basic understanding of turbulent flows.

The PDF transport equation for incompressible flow:

$$\frac{\partial f}{\partial t} + V_i \frac{\partial f}{\partial x}$$

$$R_{\text{eff}}\frac{\partial u^{(i)}}{\partial t} + R_{\text{eff}}v^{(j)}\left[\frac{\partial u^{(i)}}{\partial \xi^{(j)}} + u^{(k)}\Gamma^{i}_{kj}\right] = -R_{\text{eff}}\left[g^{(ij)}\frac{\partial P}{\partial \xi^{(j)}} - \frac{\partial v_E}{\partial \xi^{(j)}}\left[g^{(jk)}\frac{\partial u^{(i)}}{\partial \xi^{k}} + g^{(jk)}\Gamma^{(i)}_{(lk)}u^{(l)} + g^{(ik)}\frac{\partial u^{(i)}}{\partial \xi^{k}} + g^{(ik)}\Gamma^{j}_{lk}u^{(l)}\right.\right.$$
$$\left.\left. + g^{(jk)}\left[\frac{\partial^2 u^{(i)}}{\partial \xi^{(k)}\partial \xi^{(j)}} + \frac{\partial (u^{(l)}\Gamma^{i}_{lj})}{\partial \xi^{(k)}} + \Gamma^{i}_{lk}u^{(l)}_{,(j)} - \Gamma^{l}_{jk}u^{i}_{,l}\right.\right.\right.$$

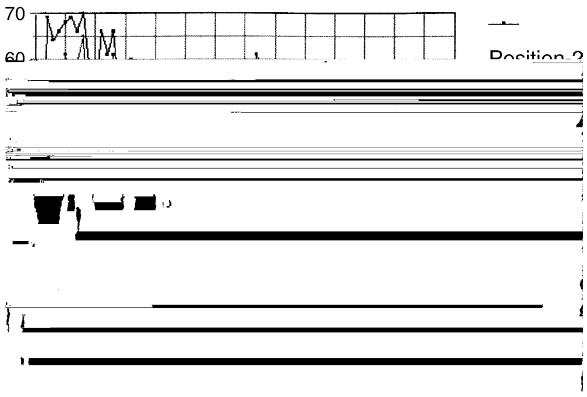

Fig. 2. Grid points concentration profiles.

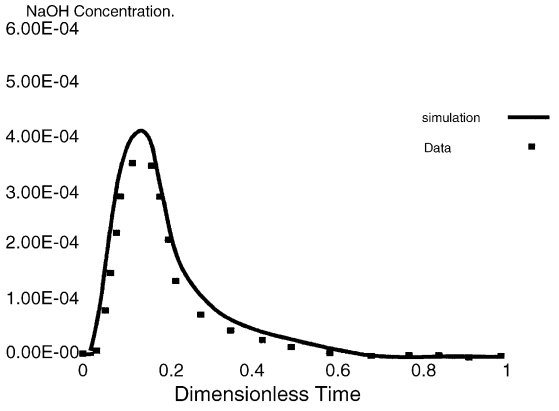

Fig. 3. Local point comparison of simulated NaOH concentration with time-averaged NaOH data at point 2 near the tip of impeller.

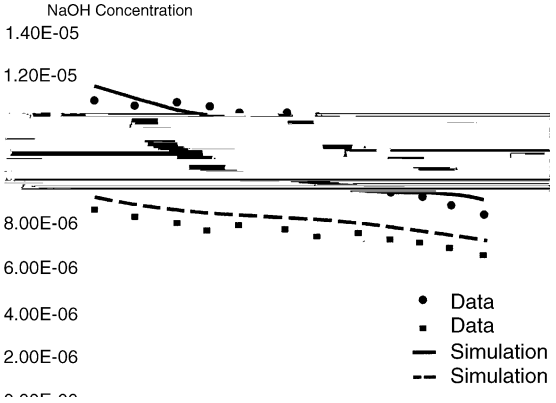

Fig. 4. Comparison of NaOH concentration as a function of dimensionless distance.

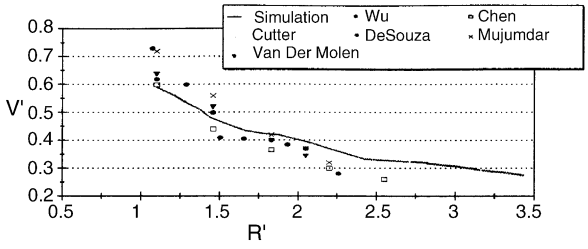

Fig. 5. A radial velocity profile in the impeller stream.

methods, the liquid flowrate and thermodynamic state exiting the injector element and the geometry and thermal structure of the wall are available as boundary conditions. Although spray flames have been investigated by experiment and analysis for more than 30 years, practical simulations of launch vehicle engines are not possible. These investigators proposed and sought validation for an engineering model, which provided the desired design tools.

The major problem in simulating dense spray flames is that the particle size and distribution created by the individual injector elements cannot be measured. This means that postulated spray formation models cannot be validated with respect to the initial mixing of the spray droplets. These investigators devised a new model of these processes based on reasonable, albeit approximate, physics of the spray. Many large rocket engine combustors operate at supercritical conditions; hence, even if droplets are present they would be unstable. Had the entering propellants been assumed to be gases, the local propellant enthalpy and mixing conditions would be erroneously simulated. Yet, such simulations have been used by the industry since the early 60s. The new spray model utilized a mature CFD code for turbulent, reacting flow and approximated the spray to be a homogeneous, real fluid whose thermodynamic properties accounted for the multi-phase flow effects. Thus, the local amount of liquid propellant was described in terms of the fluid quality. Initially, there was assumed to be no velocity or thermal lag between the phases. The plan was that: (1) thermal lags could be represented by "kinetics" models which delayed the transition of liquid droplets to gaseous globules and (2) that spray mixing rates could be adjusted by modifying the empirical turbulent transport coefficients to fit what ever data was to be used for the validation process. This spray model was implemented and tested by comparison to available test data. In short, the validation showed that the model was very reasonable with no modifications needed to account for thermal lags or mixing behavior. Even though the simulations were computationally intensive, the chamber mixing and local heat release in terms of injector design parameters were predictable for the first time. Subsequent improvements to the computational efficiency are being addressed. More importantly, testing parameters can now be identified which when measured can lead to improved simulation methodology.

Details of this new spray combustion model for high-pressure flames is described as follows. The FDNS–RFV CFD code was used to solve a set of non-linear, coupled conservation equations. Finite differences were employed to discretize the equations on a non-staggered grid. High-order up-wind, total variation diminishing (TVD) or second-order central differencing with second- or fourth-order dissipation was used to represent convective terms and stabilize shock structure, if any. Second-order central differencing was used to represent viscous and source terms. Vectorized point implicit, conjugate gradient, and generalized minimal residual matrix solvers were optionally employed to insure a stable, accurate, and fast convergence rate. Multi-block, multi-zone options were included to efficiently represent complex geometries. A pressure based predictor/multi-corrector was employed so that both compressible and incompressible flows could be simulated. A time-centered Crank–Nicholson or Euler implicit time-marching scheme was used for time-accurate discretization. For steady-state simulations, implicit Euler or explicit marching may be used. Options to account for either finite-rate or equilibrium chemistry are included. Real fluid properties are obtained from thermal and caloric equations of state. Turbulence is represented with either an incompressible (i.e. constant density) or compressible, two-equation κ–ε model. Wall boundary conditions may be satisfied with direct integration to the wall or with wall functions.

The conservation equations solved in the general curvilinear coordinate system employed are as follows:

$$\frac{1}{J}\frac{\partial}{\partial}(pq) + \frac{\partial}{\partial}(\rho U_i q) = \frac{\partial}{\partial}\left[\mu_e G_{ij}\frac{\partial q}{\partial}\right] +$$

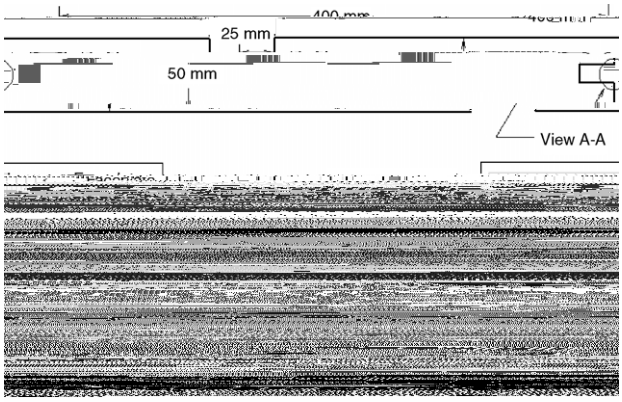

Fig. 6. Configuration and inlet flow conditions of the RCM-2 test case.

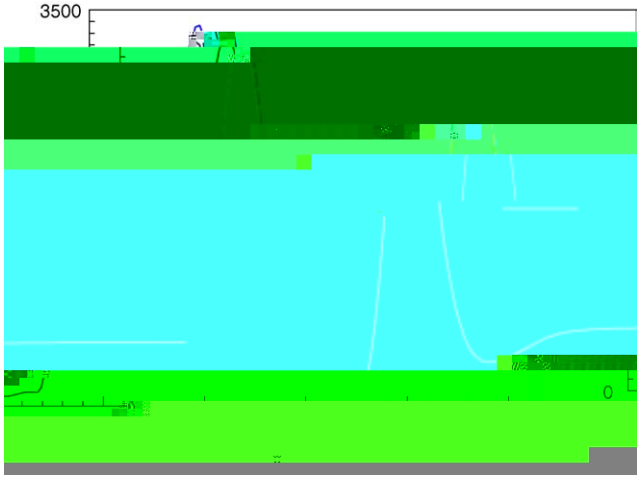

Fig. 7. Comparisons of temperature profile at $x/y = 2$, RCM-2 test case.

reaction schemes assumed all of the oxygen to be reacting with the hydrogen. Since the rate of reaction of LOX and gaseous hydrogen is not known, a third simulation was made. The LOX and GOX were assumed to be two separate species, and only the GOX was allowed to react (either to equilibrium or at a finite-rate). The split between LOX and GOX was made along an isotherm somewhat warmer than the critical isotherm, thus, some dense vapor was treated as liquid. Withholding the LOX

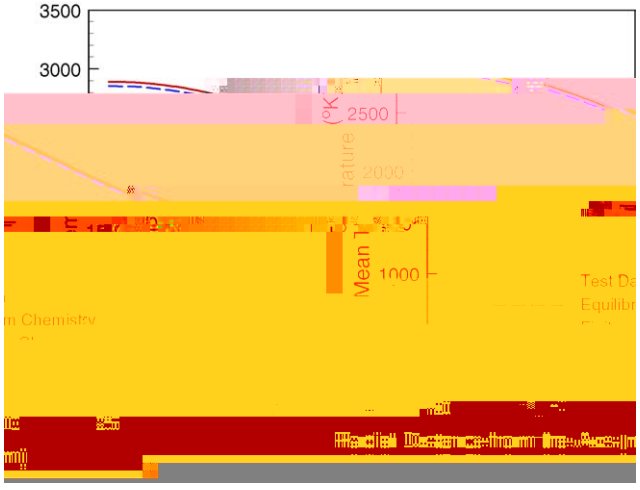

Fig. 9. Comparisons of temperature profile at = 50, RCM-2 test case.

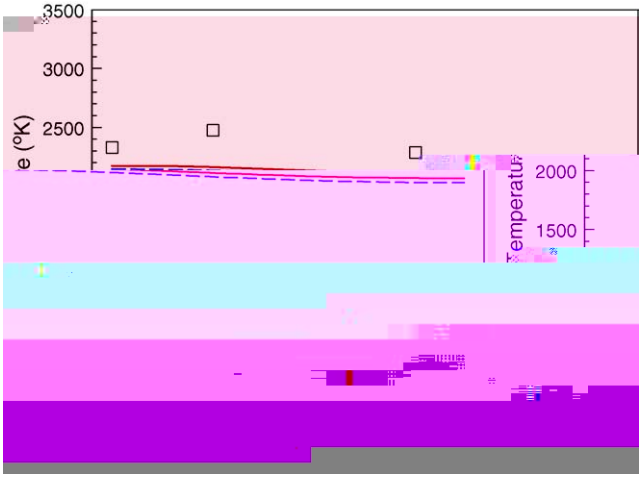

Fig. 10. Comparisons of temperature profile at = 82, RCM-2 test case.

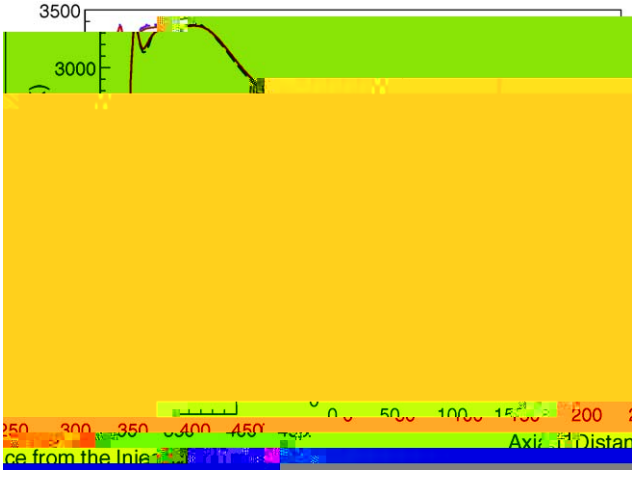

Fig. 11. Comparisons of temperature profile at = 2, RCM-2 test case.

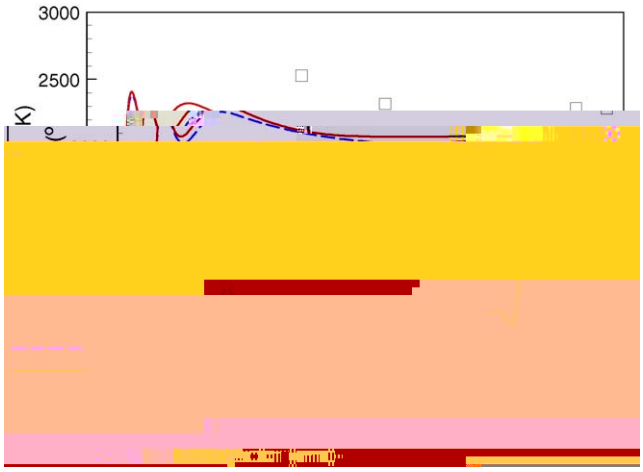

Fig. 12. Comparisons of temperature profile at = 3, RCM-2 test case.

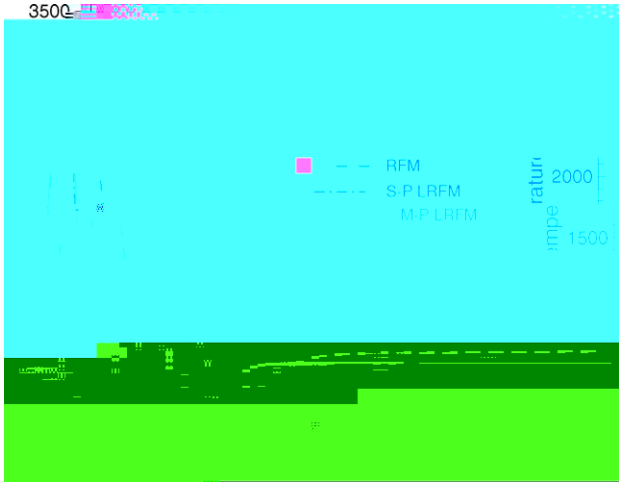

Fig. 13. Effect of omitting LOX reactions.

from the reaction fit the data better near the faceplate, as shown in Fig. 13. The withheld LOX cases fit the downstream profiles differently. The case withholding the LOX from reacting produced thinner shear layers and elongated the flame. The reported measured temperature profiles at ¥180 show which appears inconsistent with the other profile data and the simulation. The dip might not be real, but without error bounds on the measurements this cannot be ascertained. At 410 mm, the measurements are bounded by the reaction models. The dramatic effect of the two-species oxygen model on the flame shape was incidental; the change was made to improve the computational efficiency by justifying the use of the simple ideal gas model for the vast majority of grid points.

The final data shown for this case in Fig. 14 are the optical measurements of OH concentrations shown. The comparison of the magnitudes of these measurements is only qualitative, but the shape of the flame is very accurately predicted for the region near the injector face. The simulation made withholding the LOX from reacting spreads slightly faster, but the measured and simulated spread rates are about the same. This indicates that the initial predicted mixing rates are reasonable. This comparison was also made for the supercritical case with the same conclusions drawn from the exercise. The major difference in the reaction models for reacting the LOX and not doing so results in a longer flame (by about twice) for the slower combustion when the LOX is inert. However, the experimental OH map did not extend far enough downstream to verify the flame length. No temperature data were available for the supercritical case.

The treatment of the spray as a homogeneous fluid with turbulent mixing rates as established from conventional turbulence models seems to be reasonable, but critical validation data are still needed. The differences in measured radial temperature profiles, and those predicted are strongly affected by many factors in the CFD model. Whereas only the reaction model was

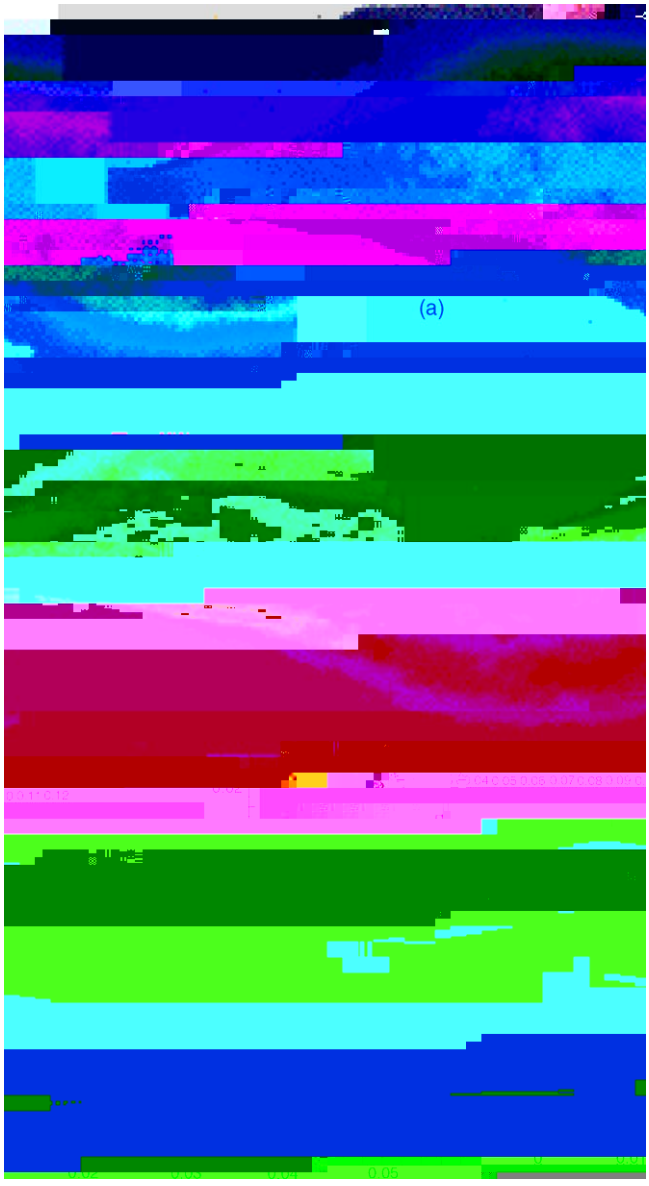

Fig. 14. Comparisons of OH concentrations, RCM-2 test case: (a) time-averaged emission; (b) Abel transformed emission; (c) numerical results.

deliberately changed, density, and turbulent mixing changed as a result. However, without error bounds on the test data further parametric variations in the simulation model would not be worthwhile. Since error bounds are difficult to establish, simple thermocouple measurements along the wall would have provided critical validation data. This is another example of losing valuable information because experiments and analyzes are not performed in concert.

The validation with the IWRCM data proved that simplified engineering analysis applied to the CFD methodology could provide a practical design tool. More validation test data are needed, but no conflicting evidence has been found that the homogeneous spray model is unrealistic. Certainly, the CFD model can be more finely tuned when new test data become available. In the mean time, the new spray combustion model is being used as a design tool to evaluate the efficiency of injector configurations. Others who have tried to model the IWRCM test data with droplet tracking models have encountered great computational inefficiency and have predicted the droplets to dribble down the centerline and not mix as rapidly as the test data indicate. The analyses described herein is the first high-pressure spray flame model that is sufficiently computationally efficient that three-dimensional injector flowfield simulations can be practically made. We cannot yet simulate the injectors with hundreds of elements. But the ability to simulate even a modest number of clustered elements is a significant advance in CFD methodology.

Fig. 15. Comparison of RCM2 jet simulations with and without LOX reactions.

7. C

(1) A wide variety of processes are represented by very similar sets of PDE conservation laws.
(2) Numerical solutions of these PDE's are practical.
(3) Accepted engineering simplifications to process analyses coupled with CFD methodology greatly increases the range of problems, which can be currently addressed.
(4) Today's CFD simulations are not trusted unless they are "validated." This is the weakness in such methodology. The "validation experiments" are most often not sufficiently similar to the prototype for the verification needed. Also, measurements are insufficient and are not made at critical locations to test the simulation.
(5) Grid generation is not taught to ChE's and Chemists.
(6) Fortran is the established computer language of transport phenomena analysts.
(7) Undergraduate ChE's and Chemists are not exposed to even an elementary CFD code.

8. R a

(1) Practical complex chemical process analysis can be accomplished with CFD simulations, which use two-equation turbulence models and conventional chemical kinetics.
(2) Using CFD methodology without access to the source code is inconvenient and risky.
(3) Establish basic computational transport phenomena code(s) to expedite modeling of complex process analyses by new practitioners.
(4) Include programming, griding, and plotting methodology instruction sufficient to utilize the CTP codes.
(5) Encourage the inclusion of computational transport phenomena methodology in ChE curricula.